4.2

A Lightning Data Assimilation Technique for Mesoscale Forecast Models

Edward R. Mansell
Cooperative Institute for Mesoscale Meteorological Studies (CIMMS)
University of Oklahoma, Norman, OK U.S.A.

Conrad L. Ziegler and Donald R. MacGorman
National Severe Storms Laboratory, Norman, OK, U.S.A.

Abstract

Lightning observations have been assimilated into a mesoscale model for improvement of forecast initial conditions. Data are used from the National Lightning Detection Network (NLDN, cloud-to-ground lightning detection) and a Lightning Mapping Array (LMA; total lightning detection) that was installed in western Kansas/eastern Colorado. The assimilation method uses lightning as a proxy for the presence or absence of deep convection. During assimilation, lightning data are used to control the Kain-Fritsch (KF) convection parameterization scheme. The KF scheme can be forced to try to produce convection where lightning indicated storms, and, conversely, can optionally be prevented from producing spurious convection where no lightning was observed. Up to 1 $\mathrm{g\,kg^{-1}}$ of water vapor may be added to the boundary layer when the KF convection is too weak. The method does not make any use lightning-rainfall relationships, rather allowing the KF scheme to generate heating and cooling rates from its modeled convection. The method could therefore be used easily for real-time assimilation of any source of lightning observations.

For the case study, the lightning assimilation was successful in generating cold pools that were present in the surface observations at initialization of the forecast. The resulting forecast showed considerably more skill than the control forecast, especially in the first few hours as convection was triggered by the propagation of the cold pool boundary.

1. Introduction

Recent studies have shown that forecasts can be improved by using a more accurate specification of deep convection during the initialization period of mesoscale forecast models. For example, from model experiments that used subjective analyses to improve initial conditions, Stensrud and Fritsch (1994a) suggested that forecasts could be improved by a data assimilation procedure that includes “the effects of parameterized convection, as indicated by radar or satellite during the assimilation period...” as well as explicit representation of boundary layer cold pools from ongoing storms as diagnosed from surface observations. Stensrud and Fritsch (1994b) demonstrated that explicitly introducing storm-induced cold pools into the mesoscale initial condition improved the mesoscale quantitative precipitation forecast by improving the triggering of ongoing convection forced by those cold pools. It is recognized, however, that data assimilation is not a panacea for all problems of forecast models. The greatest improvements in forecasts from assimilating data that depict convection should occur in environments where storms have a significant impact on near-future convection and the mesoscale environment of the convection, such as by generation of outflow boundaries and mesoscale upper tropospheric outflow (anvil) plumes (as in the case studied by Stensrud and Fritsch 1994b).

Although Stensrud and Fritsch (1994a) suggested assimilating radar or satellite data, it would be possible to use any type of data that provides the location of convection and also, preferably, a measure of its intensity. Lightning data satisfy these criteria and have the following additional advantages: compactness (i.e., low bandwidth); ability to unambiguously locate deep convection; detection in mountainous areas and beneath high cloud; and long-range detection of storms over oceans beyond radar network coverage. Furthermore, technologies capable of delineating lightning activity over the entire Earth, including over all oceans, have already been demonstrated. Thus, techniques for assimilating lightning data could be applied in extensive regions where radar coverage does not exist, such as the Pacific basin.

Relatively little has been done, however, to develop techniques for assimilating lightning data. Two studies (Alexander et al. 1999; Chang et al. 2001) demonstrated an improvement in the 12-24 hour forecast of rainfall and location of convection when lightning data were assimilated along with other satellite data during model initialization. Their assimilation scheme used occasional microwave data from a low-earth-orbiting satellite to estimate the amount of rainfall per cloud-to-ground flash, used this relationship to estimate convective rainfall during all assimilation times, converted rainfall to latent heating rates, and then used latent heating to nudge the model (Jones and Macpherson 1997). This assimilation significantly improved the forecast for the case study. Because the lightning-rainfall relationship can vary by more than an order of magnitude in warm season continental storms and by several orders of magnitude for storms in different climatological regimes (e.g., pp. 225–229 of MacGorman and Rust 1998), however, this method of assimilating lightning data would need to be calibrated for each day and region in which it is applied.

Existing technologies for satellite-based lightning mapping systems provide a more practical and secure means for global detection of thunderstorms than CG detection networks. A limitation of satellite lightning mapping systems is that they detect both cloud flashes and cloud-to-ground flashes indiscriminately. To use satellite systems, therefore, assimilation techniques must be extended to use all types of lightning. The technique of Huo and Fiedler (1998) can be extended to all types of flashes fairly easily, but does not take advantage of the additional information that can be extracted from the lightning data.

The present study uses an approach similar to those recently developed for assimilating radar data (e.g., Rogers et al. 2000) by applying data from all types of lightning in the decision process of a forecast model's convective parameterization scheme during the assimilation period leading up to the forecast period. The focus of this assimilation research is to use lightning data to activate or deactivate subgrid-scale, deep, moist convection during the data assimilation cycle of the mesoscale model. Doing this is particularly important in situations in which past convection modifies the troposphere on scales anywhere from storm scale through synoptic scale in ways that influence the subsequent evolution of convection [for example, by moistening the boundary layer, forming surface cold pools, or modifying synoptic troughs (Stensrud 1996)]. An incorrect trigger decision may have a significant adverse affect on the forecast. For example, Stensrud and Bao (1992) compared a convective parameterization trigger to a decision point in a chaotic system, and Rogers and Fritsch (1996) demonstrated the dramatic differences in rainfall estimates that can result from different trigger schemes. Therefore, corrected triggering of convection alone should have a positive impact on a forecast.

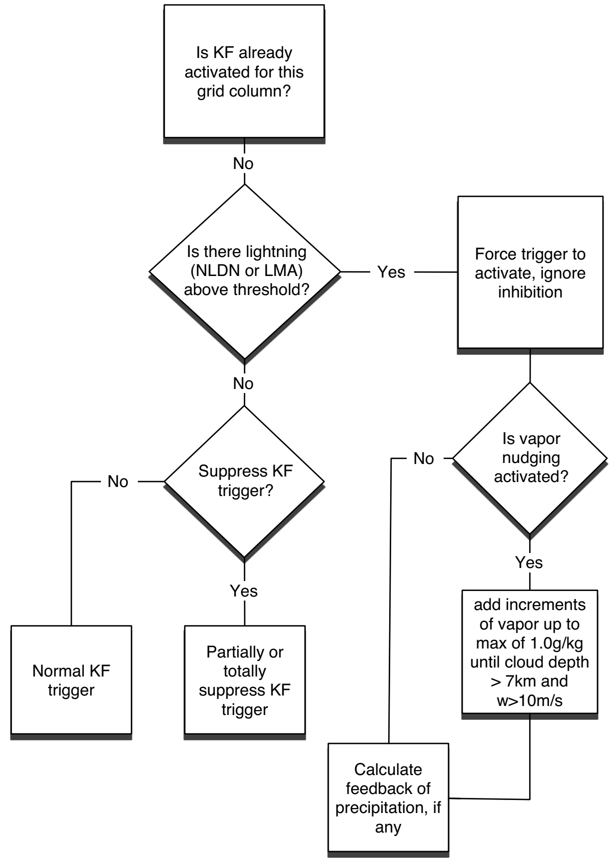

Figure 1: The decision process for each grid column during assimilation.

2. Assimilation method

The method of lightning assimilation is similar to the technique used by Rogers et al. (2000), who used radar data to determine the occurrence of convection. Lightning observations in the present technique are similarly used to control the activation of the convective parameterization scheme (CPS), which in the present work is the Kain-Fritsch (KF) scheme (Kain and Fritsch 1993; Kain 2004). This method uses the forecast model's physics to estimate the effects (including latent heating) of the deep convection inferred from lightning. This differs from the method of Alexander et al. (1999) and Chang et al. (2001), who used satellite data to estimate the rainfall per cloud-to-ground flash during the assimilation period, and then used the cloud-to-ground flash rates to determine a rate of latent heat release. Their use of latent heating replaces the convective parameterization scheme during the assimilation period.

The general outline of the decision process for assimilation is shown in Figure 1. At 10-minute intervals of model time, each grid column is checked for activation of the KF scheme. If the KF scheme is not active, the

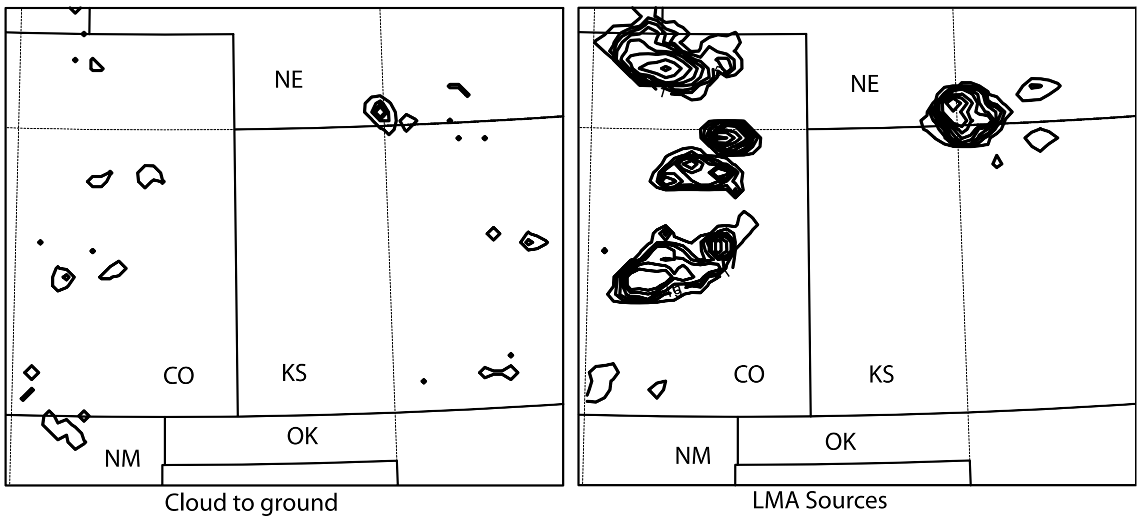

Figure 2: Lightning data for the 15 minute period starting at 21:45 UTC on 7 July 2000. a) Cloud-to-ground detections by the NLDN. b) Source points from the STEPS-LMA. Contour levels are 1, 5, 10, 20, 50, 100, 250, 500, and 1000. [The lowest level in (a) is 0.8 to make single flashes visible.]

model decides whether or not the KF scheme needs to be activated. An input threshold T_{flash} (with units of number of flashes per time interval per grid cell) is used to determine whether the observed lightning rate is locally high enough to infer the presence of deep convection. The lightning data could also be filtered for noise in the gridding process. (In future applications, T_{flash} could be made dependent on the grid spacing, as more noise points could be accumulated in a larger box.) If T_{flash} is met or exceeded during the assimilation period, but KF is not active, then an attempt is made to force KF to activate. Conversely, if the lightning counts are below T_{flash}, then KF may be hindered or completely prevented from activating, according to the selected level of suppression.

The KF trigger function tests successive mixed layers of air for instability. A mixed parcel is given some upward momentum to see if it can reach its level of free convection (LFC). If it can, then the KF model determines the cloud depth as the difference between the equilibrium level (EL) and the lifting condensation level (LCL) for that mixed parcel.

The KF scheme uses a one-dimensional updraft mass flux cloud model to determine condensation rates, latent heating and evaporative cooling rates, and precipitation rates. The scheme includes entrainment of environmental air and detrainment to the environment. The standard scheme requires a minimum cloud depth of 4 km to produce precipitation (i.e., 4 km is the threshold for deep convection). [The version of KF used here did not have the shallow (non-precipitating) convection component that is available in more recent versions.]

If forcing is indicated in a grid column by lightning during assimilation, the most unstable mixed parcel in that column is found and forced to its LFC by ignoring any negative bouyancy (convective inhibition) and entrainment below the LFC. Updrafts in storms that produce lightning, however, must be strong enough to extend well above the freezing level to produce the graupel that is necessary for strong electrification (e.g., Lhermitte and Krehbiel 1979; Holle and Maier 1982). Therefore, an option was added to increase the parcel moisture (by up to 1 g kg^{-1}) to reach a minimum cloud depth of 7 km and peak updraft of 10 m s^{-1}. The depth and updraft thresholds were chosen as reasonable values that would be attainable on average with moisture adjustments of less than 1 g kg^{-1} but greater than zero. The updraft minimum was the more stringent requirement, the depth criterion being more easily attained.

For the case in which lightning is not observed in a grid column, three options were created for suppressing KF during lightning data assimilation: (s0) no suppression, (s1) partial suppression, and (s2) complete suppression. With no suppression, the KF scheme is allowed to run without interference. Choosing the second option (s1) partially suppresses the KF scheme by limiting the “boost” given to parcels by the trigger function (thereby making it harder to reach the LFC) and by restricting the updraft width of convection in the KF scheme, which increases entrainment. By choosing the third option (s2), any grid column in which deep convection is not indicated by lightning is simply skipped by KF; the KF scheme is not allowed to run at all in that column.

A final option allowed for feedback of some convective precipitation to the resolved scaled. This option was sug-

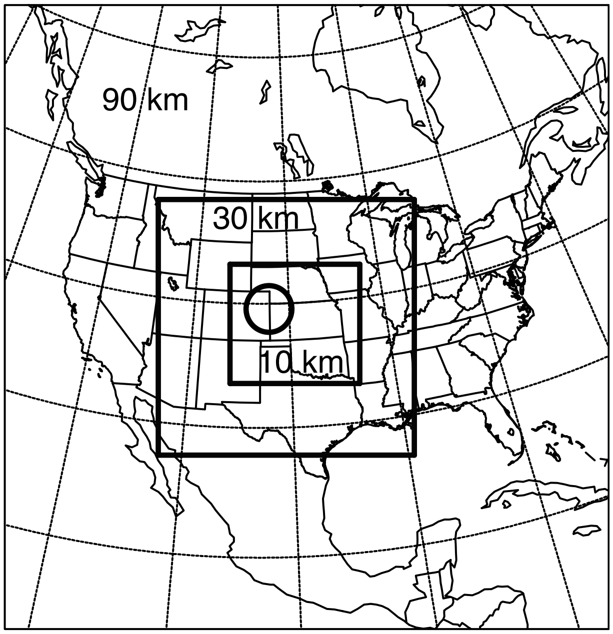

Figure 3: The coarse (90 km), intermediate (30 km), and fine (10 km) mesh areas of the model domain. The circle indicates the approximate range of the Lightning Mapping Array.

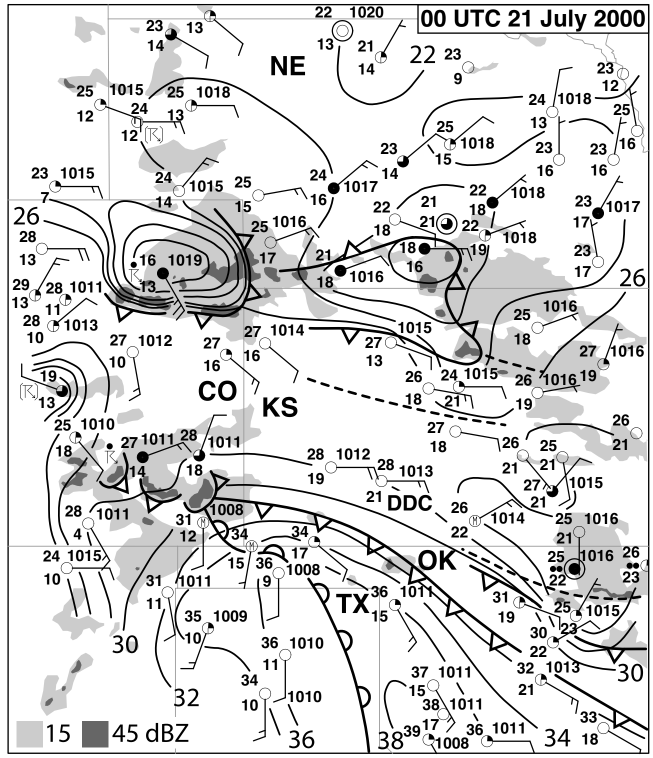

Figure 4: Surface analysis at 00 UTC on 21 July 2000, the starting time for the forecast period. Conventional station model format includes temperature (C) over dewpoint (C), mean sea level pressure (mb) at upper right, and wind barb (full barb = 5 m s^{-1}, half barb = 2.5 m s^{-1}). Instantaneous base radar reflectivity is shown by gray fill. The site of Dodge City sounding discussed in the text is indicated by DDC.

gested by J. Kain (personal communication, 2004) as a possible means to generate stronger cold pools though evaporation in the resolved-scale microphysics. Feedback is enabled during assimilation only where lightning was observed.

3. Data Sources

Lightning observations were taken from two platforms: (1) the National Lightning Detection Network (NLDN) (Cummins et al. 1998), which detects cloud-to-ground lightning over the 48 contiguous states, and (2) the Lighting Mapping Array (LMA) (Rison et al. 1999; Thomas et al. 2004), which operated in northwestern Kansas and northeastern Colorado during the STEPS field program in the summer of 2000. (STEPS = Severe Thunderstorm Electrification and Precipitation Study.) The LMA detects very high frequency (VHF) radio emissions from both intracloud (IC) and cloud-to-ground (CG) lightning flashes, but does not automatically distinguish between the two, nor does it automatically group source points into flash events. Each lightning flash may generate 10s to 1000s of source points in the LMA data.

The NLDN and the LMA provide point data that must be gridded for ingest by the model for the present assimilation scheme. The altitude information in the LMA data are ignored at present, though the full 3-D could be utilized in a future follow-on study by using a modified assimilation function (e.g., to estimate cloud depth). Satellite-based optical lightning detectors would not have altitude information, however, so an algorithm incorporating altitude would not translate to such a data source. The two lightning data sources are each gridded into separate arrays that match the domains of the nested grid configuration (e.g., as in Figure 3 for the present study). Data are accumulated for 15 minute periods over a full 12 hour update cycle, and each detected lightning point (from either the NLDN or LMA) simply increments the count in the grid box in which it falls. Other integration periods may be chosen, but the choice governs both the temporal resolution and spatial continuity of the gridded data. Fifteen minutes was chosen because it gave good temporal resolution while providing enough samples to alleviate the patchiness that can result from gridding point data.

A 'look-ahead' parameter in the assimilation routine determines how far into the future to look for the occurrence of lightning. For the present study, a look-

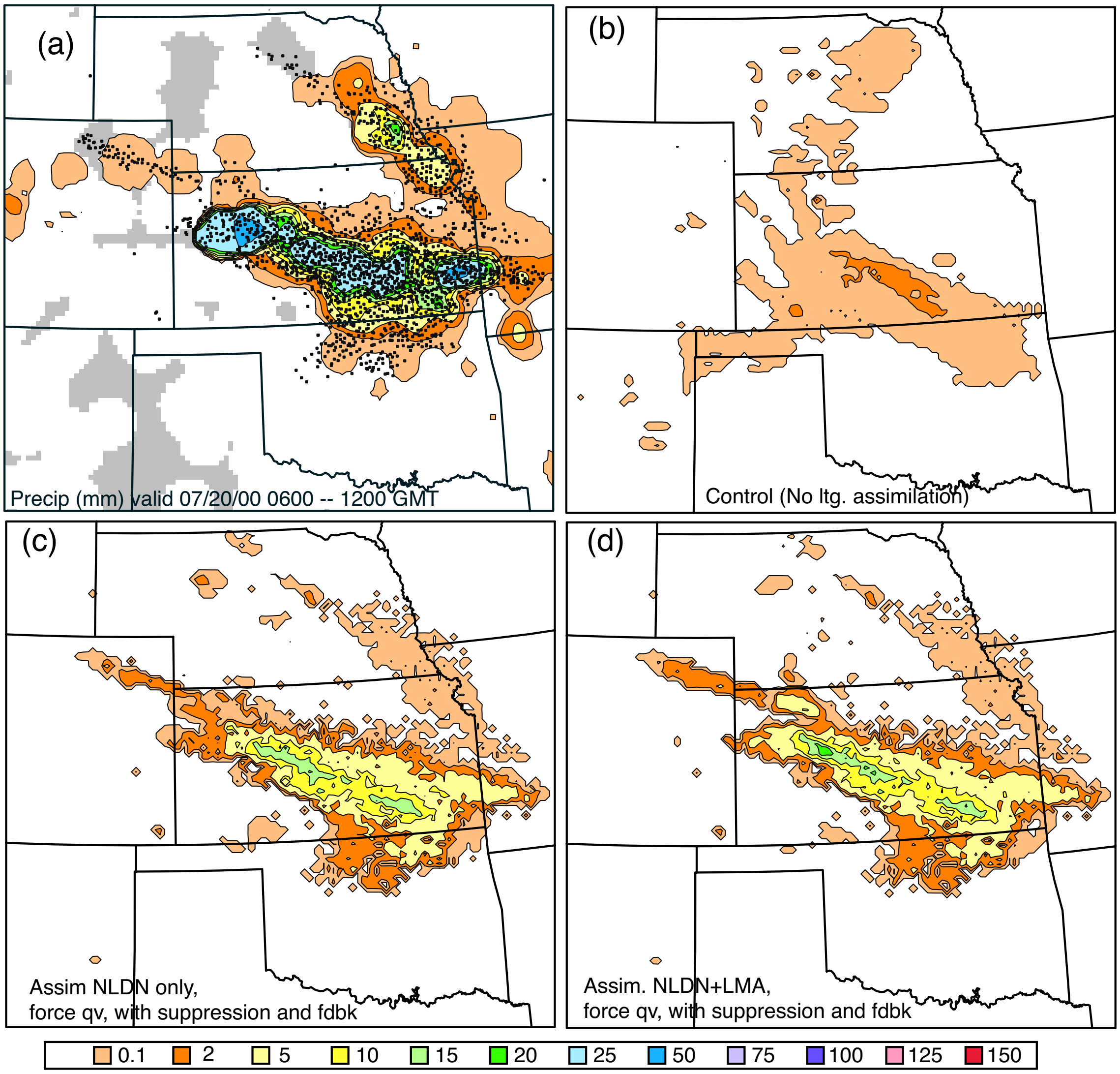

Figure 5: Observed and modeled total precipitation (mm) for a 6-hr period starting 07/20/2000 06 UTC during the spin-up period. a) Rain gauge data with sampled NLDN strikes. (The first and 30th strikes are plotted in each 10 km grid box.) Gray-filled areas indicate data voids. b) Pure forecast (no lightning assimilation). c) With assimilation of CG lightning from NLDN, moisture forcing, and full suppression. d) With assimilation of both CG and total (LMA) lightning, moisture forcing, full suppression, and 25% feedback of KF precipitation.

ahead parameter of 30 minutes was used, so that two 15-minute time periods would be aggregated and used for controlling the KF routine. (A typical time scale for KF convection is 15 to 30 minutes.) For NLDN data, the threshold T_{flash} to force KF was set at 1 strike per grid box during the look-ahead period. In the future, it may be desirable to use a threshold of 2 to avoid occasional activation of KF by spurious noise. For LMA data, T_{flash} was set at 10 points per grid box per look-ahead period, which was sufficient for removing noise points. (Some point sources with greater uncertainty could also be removed at the gridding stage, but this was not done in the present study.)

The NLDN has the advantage of large area coverage but has the shortcoming of detecting only CG lightning, which is a small fraction of all lightning (averaging roughly 25% nationally, but 10-15% over the inner grid used in this study). The coverage of the NLDN makes it a good platform for determining the occurrence of deep electrified convection, especially of long-lived large systems that produce many CG flashes. The LMA, on the other hand, detects total lightning (10s–100s of points per individual flash), but covers only out to roughly 200 km from the network center. (In the STEPS field

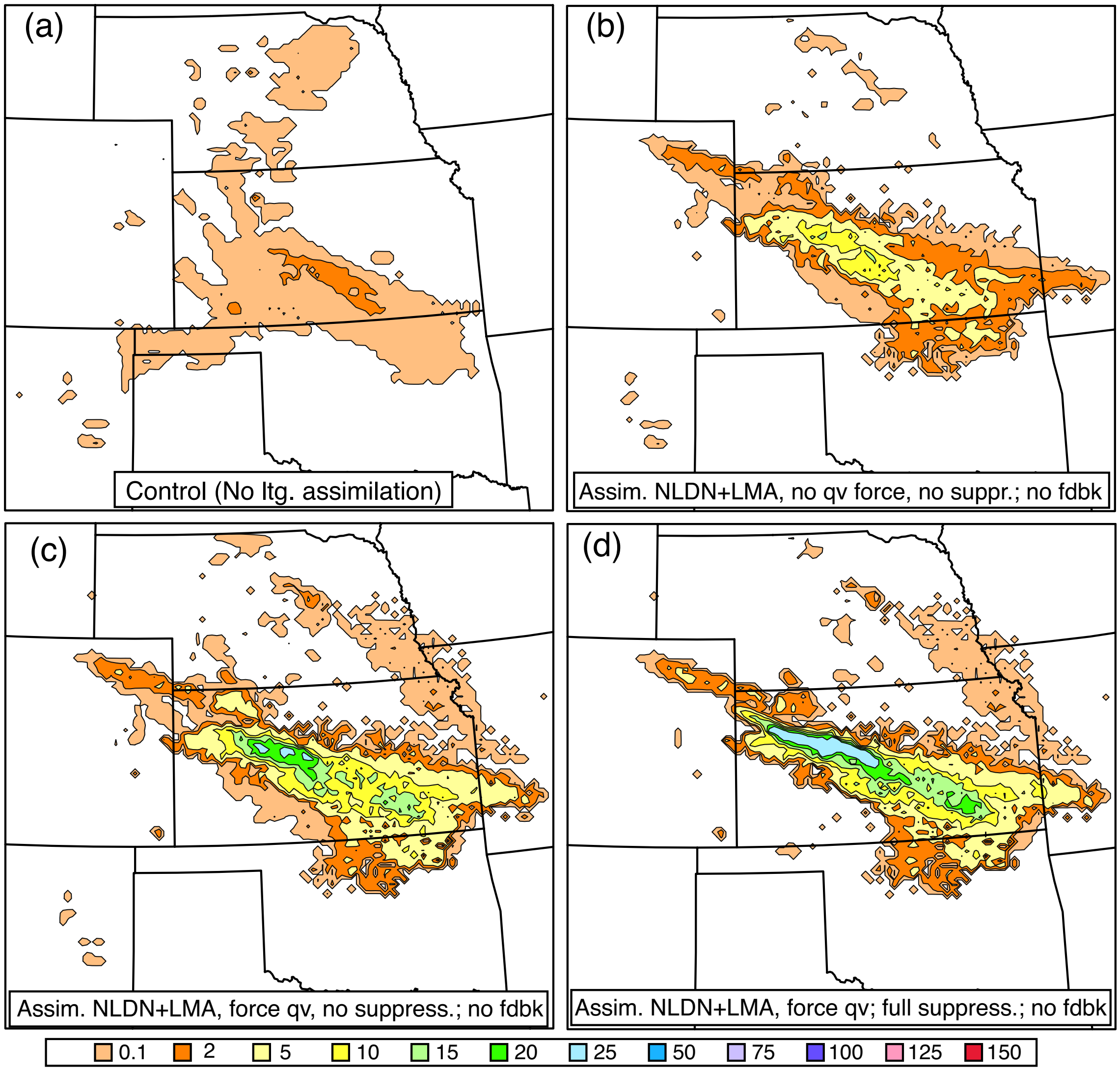

Figure 6: Modeled total precipitation (mm) for 06–12 UTC 07/20/2000 (during the spin-up period). These simulations have no precipitation feedback from the CPS to the resolved scale. a) as in Figure 4b (control run). b) Normal KF trigger with forcing from lightning assimilation. c) as for (b) adding nudging of boundary-layer moisture. d) as for (c) but suppresses the KF trigger where no lightning occurred (no precipitation feedback). The region of heaviest rainfall in (d) has a substantial resolved-scale contribution.

program, the network center was in far northwestern Kansas.)

An example of NLDN and LMA data for a 15 minute period during the case study period illustrates typical differences in the detail of the ongoing convection available from each source, as well as the spatial coverage of the two networks (Figure 2). The LMA data have far greater detail, giving a better picture of the electrical intensity, cellular structure, and coverage of individual storms within the LMA detection range (eastern Colorado, western Kansas, and southwestern Nebraska). The NLDN indicated storms in central Kansas and northern New Mexico that were out of LMA coverage. Storms in the high plains region of the U.S. tend to have a lower percentage of CG flashes than the U.S. average (e.g., Boccippio et al. 2001), so the difference shown in the figure may be greater than typical of other regions. Since the LMA detects total lightning, it can more accurately determine the timing of initial strong electrification than the NLDN, because the first flashes in storms are usually IC discharges.

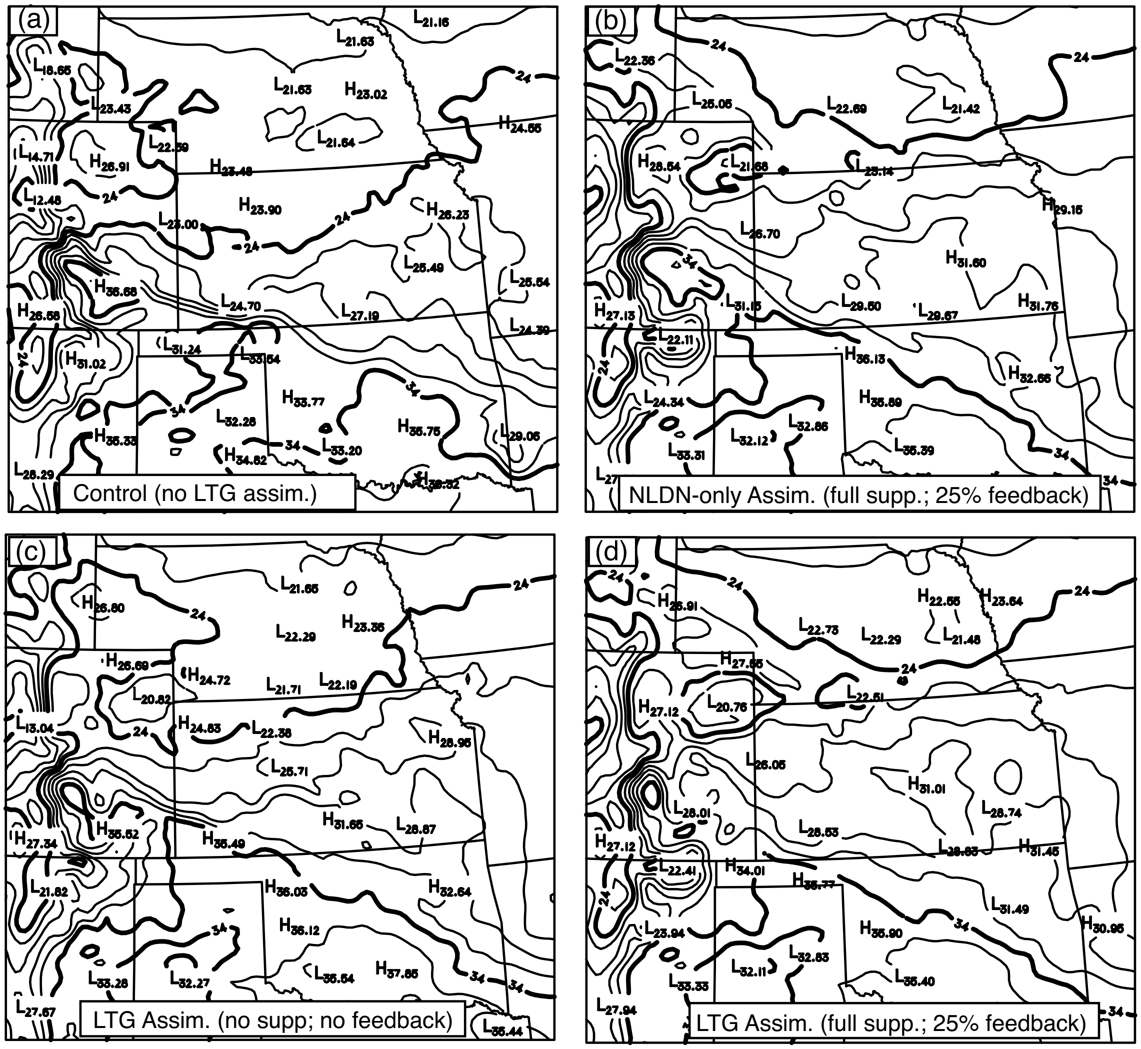

Figure 7: Air temperature (2 m) at 00 UTC on 21 July 2000, the beginning of the forecast period. (a) Warm start with 24-hr spin-up, 12-hourly data update cycle. (b) 24-hr assimilation of NLDN only with full suppression and 25% feedback of precipitation from KF to the resolved scale. (c) 24-hr assimilation of all lightning (NLDN and LMA) data to force convection (no suppression of KF nor feedback of precipitation). (d) As for b but with assimilation of both NLDN and LMA data.

4. Model Setup and Initialization

The lightning assimilation technique was developed for and applied to the COAMPS$^{\mathrm{TM}}$ (version 2) mesoscale model (Hodur 1997) in research mode. All model runs in the present study employed a CONUS-scale outer grid and two finer-scale nested domains (Figure 3) having grid spacings of 90, 30, and 10 km. Thus, resolvable scale on the innermost grid implies the full representation of meso-β scale (about 20 km to 200 km) circulations associated with a forecasted mesoscale convective system or MCS (Ziegler 1999). The innermost grid covered the STEPS program region and most of the area affected by the observed convection. The simulations all had 30 sigma-z levels, with the uppermost mass point at 31.05 km and the uppermost w-point at 34.8 km.

The Kain-Fritsch CPS was enabled on all grids, and COAMPS was initiated at 00 UTC on 20 July 2000 (cold start) from analyses, with boundary conditions from NOGAPS. The 24-hr spin-up period was performed for all forecasts, including a 12-hourly ingest of atmospheric observations via the built-in multivariate optimal interpolation (MVOI). For all experiments other than the control run, lightning data assimilation options were enabled during the spin-up period. For lightning cases, assimilation of NLDN data was always enabled on the outermost grid. Suppression of KF was never chosen for the outermost grid, because it extended beyond the range of the

NLDN. The middle grid, however, always had the same KF suppression option as the innermost grid. Due to the limited spatial coverage of the LMA, its data were assimilated only on the innermost grid, always with NLDN data being assimilated, too. A 12-hr pure forecast was then initiated from warm-start conditions at 00 UTC on 21 July 2000.

5. Case Study

The lightning assimilation method was tested with a case from July 2000 in the U.S. central plains. The STEPS field program operated in the region of western Kansas, eastern Colorado, and southwest Nebraska, and a lightning mapping array (LMA) covered approximately a 200-km radius centered near the Kansas-Colorado border (Figure 3). Widespread convection occurred on each of successive days (20 to 22 July 2000). On each day, convection initiated in Colorado and/or Nebraska and developed into convective systems that traversed Kansas into Oklahoma, Missouri and Arkansas. Convection also developed in a similar manner on 19 July, but was not as extensive or long-lived.

Since the major objective of the study was to improve the forecast initial condition through the generation of cold outflow boundaries from previous convection, a 24 hour assimilation spin-up period was run from 00 UTC on 20 July through 00 UTC on 21 July 2000. On 20 July, deep convection had initiated in eastern Colorado by 00 UTC, and squall lines had developed in Nebraska and Kansas by 06 UTC. By 12 UTC, a large system covered southeastern Kansas and parts of Oklahoma and Missouri. The system moved into Missouri and Arkansas by 16 UTC, and new storms began forming in Colorado and Kansas by 20 UTC. A vigorous system was in place in northeastern Colorado by 00 UTC 21 July, with convection also evident in southern Colorado and north-central Kansas/south-central Nebraska (Figure 4). The spin-up period thus had both earlier convection and new, ongoing convection and a combination of old and new outflow boundaries (Figure 4).

6. Results during Assimilation

a. Precipitation

Lightning data assimilation substantially improved the location and amount of precipitation during the spin-up period. Figures 5 and 6 display the precipitation accumulation during the period 06 to 12 UTC (20 July 2000) as reported by rain gauges and from different forecast experiments. The gauge data are from the Stage IV NCEP rainfall analysis (Baldwin and Mitchell 1998; Fulton et al. 1998; Seo 1998). (The multi-sensor product was not available for this case.) The control run (Figure 5b) had the least (and so worst) rainfall amounts, although the

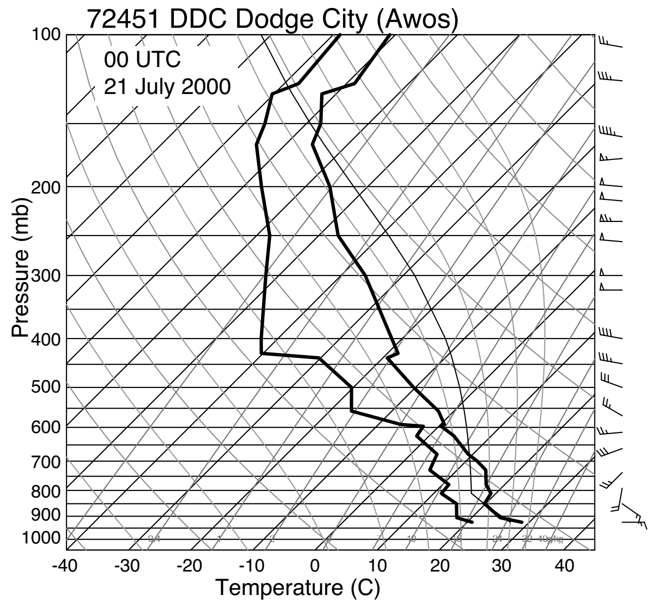

Figure 8: National Weather Service sounding for Dodge City, KS, at 00 UTC on 21 July 2000.

greatest values being placed accurately with the larger observed rainfall values in Kansas suggests some skill on the part of the base model. The lightning assimilation cases produced more rain in Kansas as well as capturing some convection in southeastern Nebraska and northeastern Kansas. Water vapor nudging was able to substantially enhance the amounts of precipitation (compare Figures 6b and 6c), but the rainfall was still less than was observed. The quantitative precipitation estimate during the lightning assimilation period was up to approximately 40% of observed precipitation amounts. This supports the conclusion that forcing subgrid convection when lightning is present maintains much more realistic intensity and coverage of convection.

Although assimilating NLDN ground strike data alone provided considerable improvement (Figure 5c), some further improvement occurred when LMA total lightning data were assimilated with NLDN ground strike data (Figure 5d). The addition of LMA data enhanced rainfall in western Kansas. The enhancement may appear to be a little too much in the extreme northwestern part of the state, but the rain gauge network may have poorly sampled those isolated storms.

Suppressing convection from the KF scheme where no lightning was observed helped to remove the spurious precipitation seen in the control forecast in Nebraska and in the Oklahoma panhandle region. The experiments that did not actively suppress KF were also able to reduce the frequency of spurious convection (Figure 6b,c) that was present in the pure forecast mode, possibly

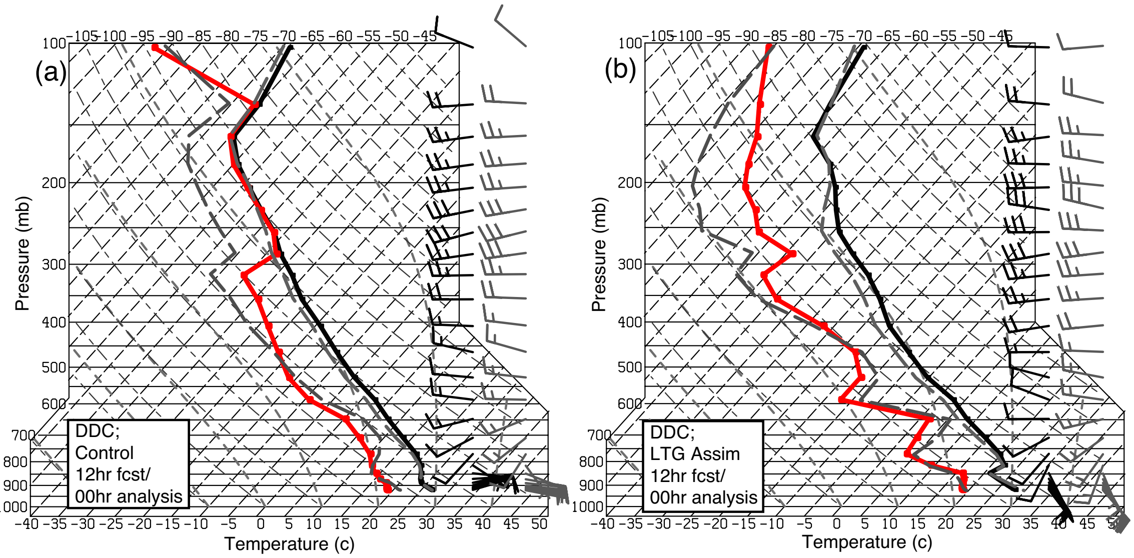

Figure 9: Model soundings for Dodge City, KS, at 00 UTC on 21 July 2000. Red and black curves show dewpoint and potential temperature, respectively, of the 12-hr forecast. Long dashed curves are the adjusted values after the initialization of the next forecast cycle. Black wind barbs are from the forecast, gray barbs are from the subsequent analysis adjustment. (a) Control run (no lightning assimilation). (b) Simulation with assimilation of lightning (NLDN and LMA), full suppression, and 25% feedback of precipitation from the KF scheme to the resolved scale.

because assimilation improved the boundary conditions provided from the outer grids or from the effects of earlier forced convection.

b. Effects on forecast initial conditions

A particular interest of this research is the generation of mesoscale boundaries by convective outflows. Surface and WSR-88D radar mosaic observations at 00 UTC on 21 July indicate a strong, cold outflow forced by convection in northeastern Colorado, as well as boundaries in southeastern Colorado, north-central Kansas, and across Oklahoma (Figure 4). The surface temperature fields from four model experiments are shown for comparison in Figure 7. (A cold-start analysis had an obvious cold bias and is not shown.) The control case (Figure 7a) did not generate the observed convection in northeastern Colorado during the spin-up period and, therefore, failed to build the observed surface cold outflow.

A clear difference from the control run is seen in the experiments with lightning assimilation (Figures 7b,c,d): a convectively-generated cold pool is evident in northeastern Colorado as seen in the surface analysis. The case with assimilation of NLDN data only (Figure 7b) developed a cold pool where convection was observed in northeastern Colorado, but it is weaker than when the same options were used with total lightning assimilation (NLDN plus LMA; Figure 7d). This is a result of the sparseness of the NLDN ground strikes compared to the LMA total lightning data (seen in Figure 2). In the two examples with total lightning assimilation, a stronger thermal gradient around the cold pool can be seen in the experiment in which spurious convection was actively suppressed (compare Figures 7c and 7d).

Soundings at Dodge City, KS, (DDC) also illustrate differences in the initial conditions generated by the control and assimilation experiments. The National Weather Service sounding from DDC at 00 UTC on 21 July 2000 is plotted in Figure 8 (the sounding location is shown in Figure 4). Model-generated soundings at the DDC location are shown in Figure 9 from before and after the MVOI analysis. The control run sounding was saturated from 300 mb up to about 175 mb due to anvil outflow of spurious convection to the southwest of DDC. On the other hand, the sounding from the lightning assimilation case is drier and more unstable above the moist boundary layer in agreement with the observed sounding (i.e., it does not exhibit contamination by convection) and, except for the near-surface winds, compares more favorably with the observed sounding. The homogeneously mixed elevated residual layer (ERL) above the moist boundary layer in the lightning assimilation sounding probably would have been rather more mixed along a moist virtual adiabat, in agreement with the observed profile under the action of a cumulus field, had the shallow cumulus convection component of the KF scheme been available and activated.

Examination of ground layer conditions in the model

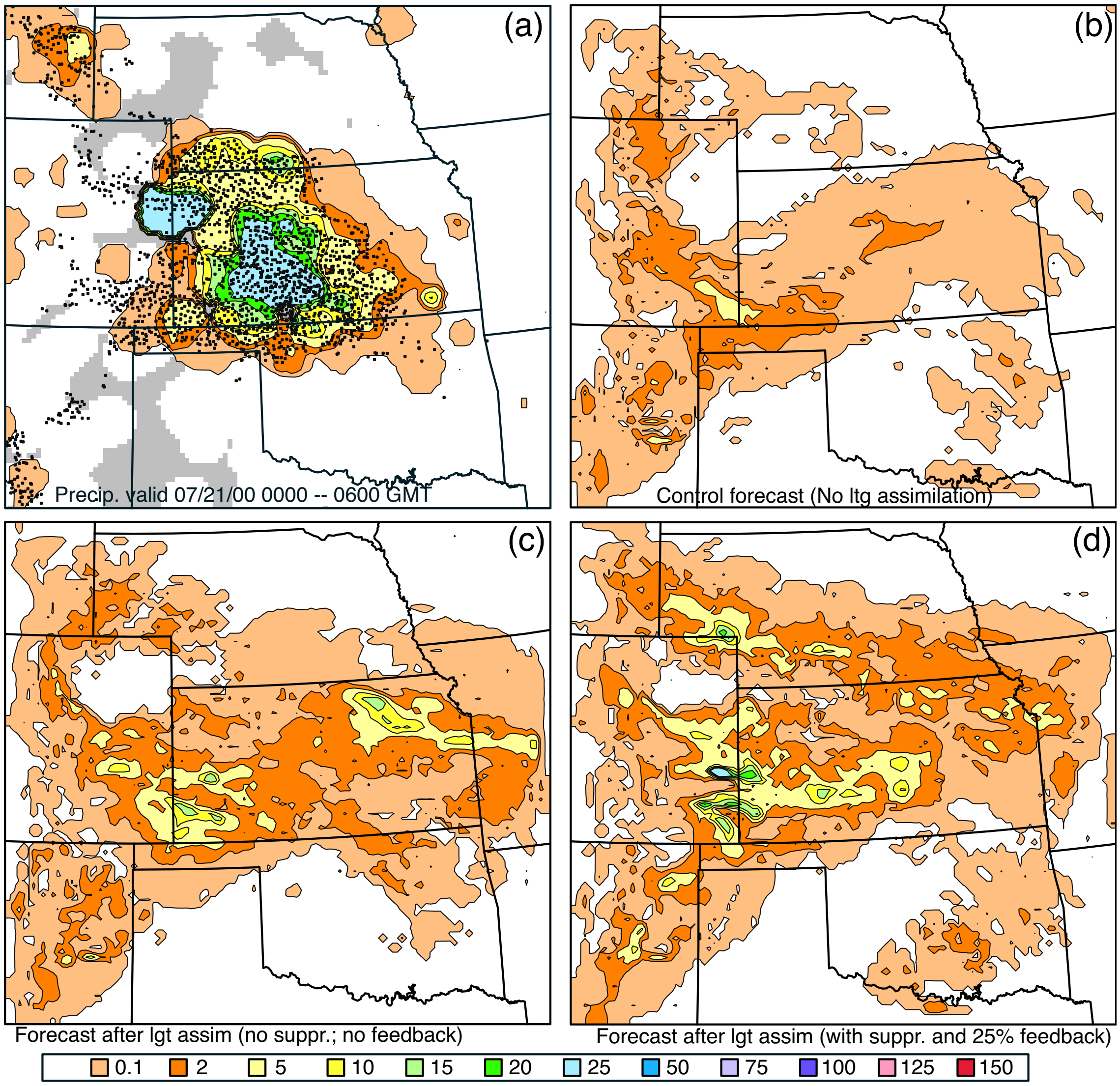

Figure 10: Observed and forecast total precipitation (mm) for 00–06 UTC on 07/21/2000. (a) Rain gauge data with sampled NLDN strikes. (The first and 30th strikes are plotted in each 10 km grid box.) Gray-filled areas indicate data voids. (b) Pure forecast from standard warm start (no lightning assimilation). (c) Forecast from initialization with assimilation of NLDN and LMA data, moisture forcing, and no suppression nor feedback. (d) Forecast from initialization with assimilation of both CG and total (LMA) lightning, moisture forcing, and full suppression and 25% feedback.

output data (not shown) indicate that increased convective and total precipitation caused a significant increase in soil moisture in areas of antecedent convection. Given the demonstrated ability of assimilating lightning data to improve quantitative precipitation estimates during the assimilation period, soil moisture availability is then theoretically more reliable in areas which had received heavy precipitation. The spatial soil moisture availability field is highly relevant to the determination of mesoscale surface layer fluxes (Marshall et al. 2003). Local soil moisture variations due to factors such as previous convective precipitation may assist in forcing boundary layer evolution and convective initiation during subsequent diurnal cycles (e.g., Ziegler et al. 1995, 1997).

7. Results: Forecast

A main hypothesis for this study was that correctly locating soil moisture and outflow boundaries for the initial condition should improve model forecasts by improving the placement of physical mechanisms for triggering convection. Lightning data assimilation was successful in reproducing observed cold outflow, so the remaining

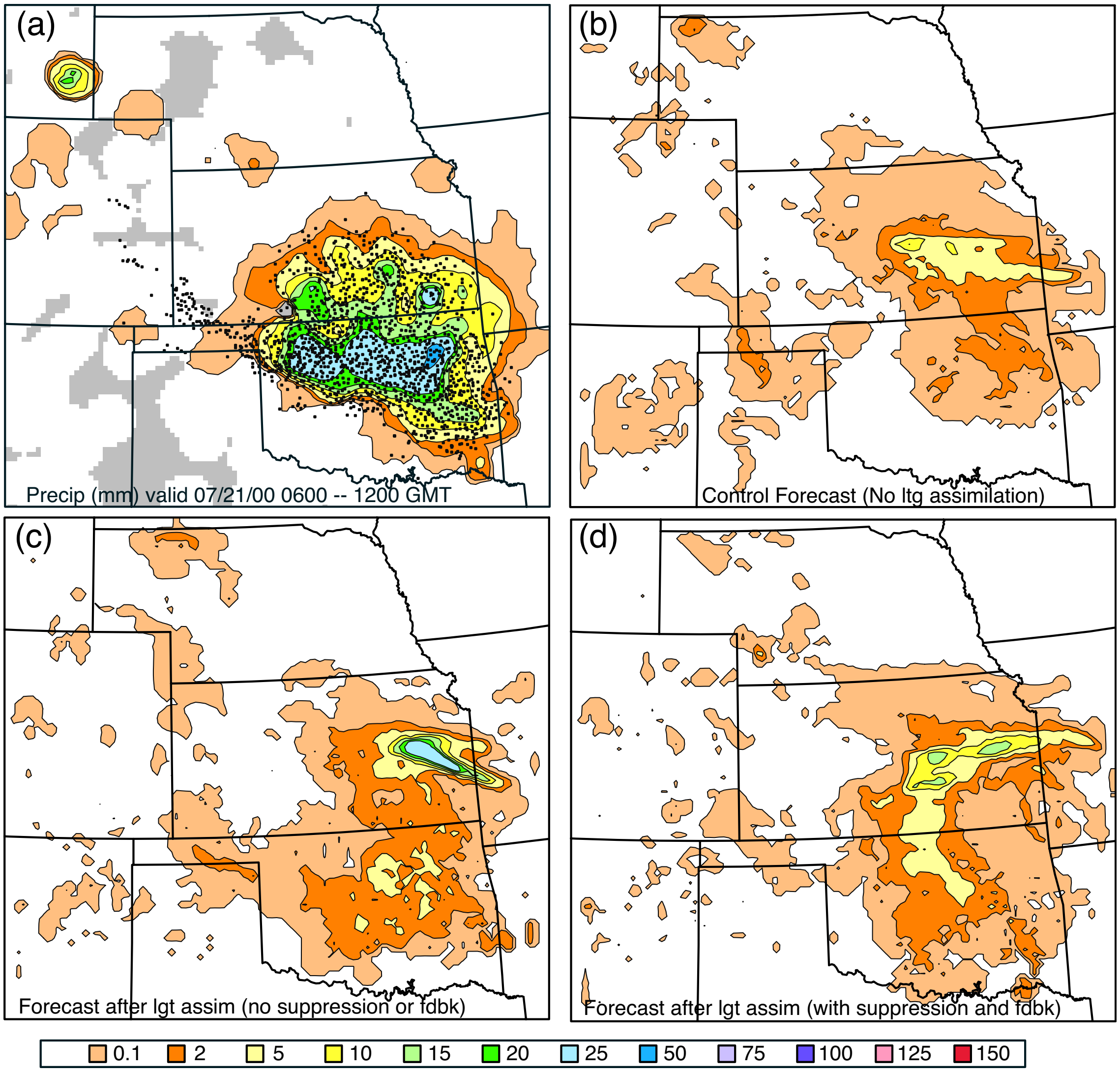

Figure 11: Observed and forecast total precipitation (mm) for 06–12 UTC on 07/21/2000. (a) Rain gauge data with sampled NLDN strikes. (The first and 30th strikes are plotted in each 10 km grid box.) Gray-filled areas indicate data voids. (b) Pure forecast from standard warm start (no lightning assimilation). (c) Forecast from initialization with assimilation of NLDN and LMA data, moisture forcing, and no suppression nor feedback. (d) Forecast from initialization with assimilation of both CG and total (LMA) lightning, moisture forcing, and full suppression and 25% feedback.

test is whether forecast skill was improved.

Observed and forecast rainfall accumulations for 6-hr forecast periods are shown in Figure 10 (00 to 06 UTC on 21 July 2000) and Figure 11 (06 to 12 UTC). The larger observed rainfall accumulations from 00 to 06 UTC stretched from east-central Colorado and northwestern Kansas to south-central Kansas (Figure 10a). The forecasts based on lightning assimilation (Figure 10b,c) produced a more accurate pattern and quantity of the larger rainfall accumulations than the control forecast in this region. The assimilation-based forecast that did not suppress the KF scheme (Figure 10c) had less spurious convection in Nebraska than the other experimental forecast, but it also had a greater overestimate of rainfall in northeastern Kansas.

In the second six-hour period of the forecast, from 06 to 12 UTC, the heaviest observed accumulations had moved into Oklahoma, and relatively large values extended into south-central and southeastern Kansas (Figure 11a). By this period, the pattern and amount of rainfall accumulations in Kansas from the experimental forecasts were converging on the pattern from the con-

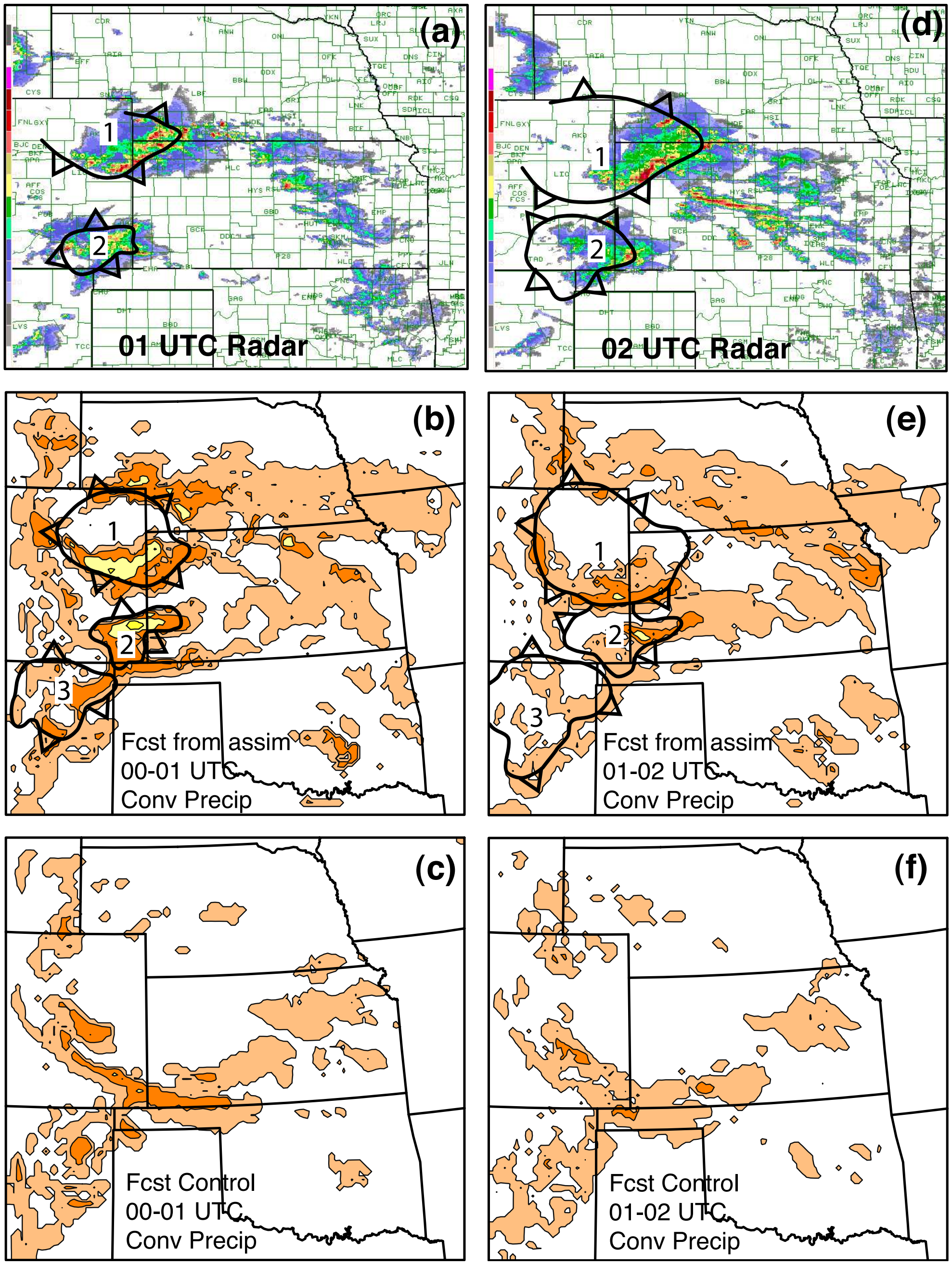

Figure 12: Radar composites and convective precipitation forecasts on 21 July 2000. (a) Radar composite at 01 UTC. (b) 00-01 hour precipitation forecast from initial condition generated by assimilation of both CG and total (LMA) lightning, moisture forcing, and full suppression and 25% feedback. (c) 00-01 hour control forecast from standard warm start (no lightning assimilation). (d, e, f) As for (a, b, c) but for 02 (01-02) UTC. Observed and forecast cold pool boundaries are overlaid, the latter determined from the forecast surface temperature field associated with convective rainfall cores. For reference, reflectivity at 00 UTC was depicted in Figure 4.

trol forecast, but in Oklahoma, the pattern and amounts of rainfall from the experimental forecasts were still improved in comparison with the control run. Although the experimental forecasts were at least somewhat better than the control forecast throughout the period, the larger values of rainfall accumulation in the experimental forecasts, dominated by subgrid-scale convective precipitation, became a smaller fraction of the observed accumulations with time, from roughly 20% of the larger observed accumulations at 00-06 UTC to roughly 10% of the larger observed accumulations at 06-12 UTC.

This decrease in the forecasted rainfall accumulation relative to observations can be understood better by focusing on the early hours of the 00-06 UTC forecast period. A comparison of the hourly evolution of the observed radar reflectivity and cold pools with that of the forecasted convective rainfall and the associated cold pool boundaries shows that assimilation of lightning data into the initial conditions did, in fact, improve the first several hours of the forecast mesoscale evolution (Figure 12).

The observations show that a convective line from northeastern Colorado (cold pool 1 in Figures 12a,d) propagated roughly toward the southeast, with other storm elements going eastward just north and south of the Kansas-Nebraska border. The observed storms in southeast Colorado (cold pool 2) weakened slightly and moved to the east over the two hour period. At 02 UTC, the radar showed a hint of an outflow boundary heading southward though east-central Colorado. Cold pool 3, associated with other forecast convection in northeast New Mexico, could not be evaluated because of sparse surface observations and radar blockage by terrain.

The control forecast (Figure 12c,f) failed to generate any significant convection in northwestern Kansas or along the Kansas-Nebraska border, but produced convection along a temperature gradient that arched through southeastern Colorado and extended farther into southwestern Kansas than observed (Figure 7b). In the experimental forecast (Figure 12b,e), on the other hand, propagation of the two outflow boundaries (1 and 2) was similar to the observed behavior. [This improvement is analogous to the improvement found by Pereira Fo. et al. (1999) when they assimilated rainfall rate data to initialize a mesoscale forecast model.] During the first hour, convection was triggered by the assimilation-produced cold pools in eastern Colorado, southwestern Nebraska, and northwestern Kansas, much as was observed.

The main convective line produced in northeast Colorado by the assimilation propagated southward instead of southeastward, but nevertheless demonstrated more skill in forecasting this convection than the control run. The convection in southeastern Colorado was also better in the experimental forecast than in the control run, in terms of placement, rainfall amounts, and the extent of propagation eastward into Kansas. The experimental forecast, however, also had some spurious convection in Nebraska and southwestern Iowa.

The convection in the second hour of the experimental forecast weakened relative to the observed convection, because the cold pools spread out and were not sufficiently sustained by new convection in the forecast period. This weakening is particularly noticeable in the decreasing area of larger rainfall accumulations (compare Figures 12b and e), whereas the observed area of larger reflectivity was relatively unchanged (compare Figures 12a and b). Much of this weakening can probably be attributed to the already-discussed tendency for all activated subgrid-scale convection in the model to produce too little rainfall. As discussed in the last section, rainfall accumulations were only 40% of observed values, even when the convection was being nudged continually by observations, and the underestimating of rainfall increased with time in the forecast period, as shown in Figures 10 and 11. Under-forecast precipitation allows the cold pool to weaken, and so also weakens the subsequent triggering of convection by the cold pool. This insufficient feedback tends, in turn, to further reduce the rainfall produced by the newly triggered convection.

8. Conclusions

Assimilating lightning data to control parameterized convection in the spin-up cycle of a forecast model has promise in improving the effects of prior convection on the initial condition of the forecast period. The most important effects of more accurate prior convective precipitation on the initial condition include more accurate representation of cold pools in the boundary layer, prevention of convective contamination of the environment where convection did not occur, and a more accurate distribution of soil moisture availability. The results suggest an optimal approach wherein convection is forced where lightning was observed and totally suppressed in the absence of lightning. The mere forcing of prior convection, however, can help to prevent some spurious triggering of convection in the forecast period. A continental warm-season forecast from an initial condition that included such effects of prior convection showed more skill than a control forecast, at least over a short term. The assimilation scheme implemented in this study ingests lightning data directly, without additional analysis to estimate rainfall per flash as in a prior assimilation scheme. Direct ingest makes the scheme more appropriate for use in a rapid update cycle forecast.

The results support the conclusion that forcing subgrid convection by lightning realistically maintains the intensity and coverage of convection and implies that the under-prediction of convective precipitation during the forecast period is due at least in part to difficulty in maintaining cold convective outflows and triggering new convection along cold pool boundaries. The latter difficulty in maintaining forecast storm intensity may be related to the trigger function formulation and the microphysics in the trailing stratiform (resolved-scale) region of the MCSs during the assimilation and forecast periods. Since spatial coverage is rather accurately specified during assimilation, the under-diagnosed precipitation implies either that the subgrid convection scheme inherently underpredicts convective rainfall or that the model environment has a significant dry (precipitable water) bias, or some combination of these two factors. Since precipitation is intimately connected to development and maintenance of both subgrid- and resolved-scale boundary layer cold pools in the assimilation and forecast cycles, a dry bias in rainfall amounts is consistent with accelerated weakening of the forecast MCS in our case study, compared with observations. (The observed MCS actually maintained its intensity for over 6 hours.)

The results suggest that the assimilation is most effective with total lightning data, such as from the ground-based lightning mapping array or data that could be acquired by a satellite-based optical system. Assimilating ground strike data alone does improve the initial condition of the forecast period, but not as much as assimilating total lightning data does. The reason is that ground strike data alone depict less detail and area of storm structure than total lightning data provide. It may be possible to develop a more sophisticated algorithm for using ground-strike data that would improve the NLDN-only assimilation, perhaps by using an influence radius for each CG flash.

Acknowledgements

The authors thank Dr. J. Kain for suggestions and assistance in understanding the convective parameterization. The precipitation data were provided by Dr. M. Baldwin, and thanks also to Dr. D. Stensrud for useful discussions. Thanks also to Dr. Brian Fiedler and Dr. William Beasley. Funding for this study was provided by Office of Naval Research grant N00014-00-1-0525. Support was also provided to the lead author through National Research Council associateship at the National Severe Storms Laboratory in Norman, Oklahoma. Funding for this research also was provided under NOAA-OU Cooperative Agreement NA17RJ1227. The data from the Lightning Mapping Array were provided by New Mexico Tech as part of the STEPS field program.

References

Alexander, G. D., J. A. Weinman, V. M. Karyampudi, W. S. Olson, and A. C. Lee, 1999: The effect of assimilating rain rates derived from satellites and lightning on the forecasts of the 1993 superstorm. *Mon. Wea. Rev.*, **127**, 1433–1457.

Baldwin, M. E. and K. E. Mitchell, 1998: Progress on the ncep hourly multi-sensor u. s. precipitation analysis for operations and gcip research. Preprints*, 2nd Symposium on Integrated Observing Systems*, 78th AMS Annual Meeting, Phoenix, Arizona, 10–11.

Boccippio, D. J., K. L. Cummins, H. J. Christian, and S. J. Goodman, 2001: Combined satellite- and surface-based estimation of the intracloud–cloud-to-ground lightning ratio over the continental United States. *Mon. Wea. Rev.*, **129**, 108–122.

Chang, D.-E., J. A. Weinman, C. A. Morales, and W. S. Olson, 2001: The effect of spaceborne microwave and ground-based continous lightning measurments on forecasts of the 1998 Groundhog Day storm. *Mon. Wea. Rev.*, **129**, 1809–1833.

Cummins, K. L., M. J. Murphy, E. A. Bardo, W. L. Hiscox, R. B. Pyle, and A. E. Pifer, 1998: A combined TOA/MDF technololgy upgrade of the U.S. national lightning detection network. *J. Geophys. Res.*, **103**, 9035–9044.

Fulton, R. A., J. P. Breidenbach, D. J. Seo, D. A. Miller, and T. O'Bannon, 1998: The wsr-88d rainfall algorithm. *Wea. Forecasting*, **13**, 377–395.

Hodur, R. M., 1997: The Naval Research Laboratory's coupled ocean/atmosphere mesoscale prediction system (COAMPS). *Mon. Wea. Rev.*, **125**, 1414–1430.

Holle, R. L. and M. W. Maier, 1982: Radar echo height related to cloud-ground lightning in south Florida. Preprints*, 12th Conf. on Severe Local Storms*, American Meteorological Society, 330–333.

Huo, Z. and B. Fiedler, 1998: The impacts of ADAS cloud analysis on the simulation of a coastal squall line. *Annual report to the Coastal Meteorology Research Program*, B. Fiedler, ed., School of Meteorology, Univ. of Oklahoma, 177.

Jones, C. D. and B. Macpherson, 1997: A latent heat nudging scheme for the assimilation of precipitation into an operational mesoscale model. *Meteor. Appl.*, **4**, 269–277.

Kain, J. S., 2004: The Kain-Fritsch convective parameterization: An update. *J. Appl. Meteor.*, **43**, 170–181.

Kain, J. S. and J. M. Fritsch, 1993: Convective parameterization for mesoscale models: The Kain–Fritsch scheme. *The Representation of Cumulus Covection in Numerical Models, Meteor. Monogr.*, No. 46, Amer. Meteor. Soc., 165–170.

Lhermitte, R. and P. R. Krehbiel, 1979: Doppler radar and radio observations of thunderstorms. *IEEE Trans. Geosci. Electron.*, **GE-17**, 162–171.

MacGorman, D. R. and W. D. Rust, 1998: *The Electrical Nature of Storms*. Oxford Univ. Press, New York, 422 pp.

Marshall, C. H., K. C. Crawford, K. E. Mitchell, and D. J. Stensrud, 2003: The impact of the land surface physics in the operational ncep eta model on simulating the diurnal cycle: Evaluation and testing using Oklahoma Mesonet data. *Wea. Forecasting*, **18**, 748–768.

Rison, W., R. J. Thomas, P. R. Krehbiel, T. Hamlin, and J. Harlin, 1999: A GPS-based three-dimensional lightning mapping system: Initial observations in central New Mexico. *Geophys. Res. Lett.*, **26**, 3573–3576.

Rogers, R. F., J. M. Fritsch, and W. C. Lambert, 2000: A simple technique for using radar data in the dynamic initialization of a mesoscale model. *Mon. Wea. Rev.*, **128**, 2560–2574.

Seo, D. J., 1998: Real-time estimation of rainfall fields using radar rainfall and rain gauge data. *J. Hydrol.*, **208**, 37–52.

Stensrud, D. J., 1996: Effects of persistent, midlatitude mesoscale regions of convection on the large-scale environment during the warm season. *J. Atmos. Sci.*, **53**, 3503–3527.

Stensrud, D. J. and J.-W. Bao, 1992: Behaviors of variational and nudging assimilation techniqes with a chaotic low-order model. *Mon. Wea. Rev.*, **120**, 3016–3028.

Stensrud, D. J. and J. M. Fritsch, 1994a: Mesoscale convective systems in weakly forced large-scale environments. Part II: Generation of a mesoscale initial condition. *Mon. Wea. Rev.*, **122**, 2068–2083.

— 1994b: Mesoscale convective systems in weakly forced large-scale environments. Part III: Numerical simulations and implications for operational forecasting. *Mon. Wea. Rev.*, **122**, 2084–2104.

Thomas, R. P., P. R. Krehbiel, W. Rison, S. Hunyady, W. Winn, T. Hamlin, and J. Harlin, 2004: Accuracy of the lightning mapping array. *J. Geophys. Res.*, **109**, doi:10.1029/2004JD004549.

Ziegler, C. L., 1999: Issues in forecasting mesoscale convective systems: An observational and modeling perspective. *Storms*, J. R. Pielke and S. R. Pielke, eds., Routledge Press, London, volume 2 of *Storms*, chapter 32, 26–42.

Ziegler, C. L., T. J. Lee, and R. A. Pielke, Sr., 1997: Convective initiation at the dryline: A modeling study. *Mon. Wea. Rev.*, **125**, 1001–1026.

Ziegler, C. L., W. J. Martin, R. A. Pielke, Sr., and R. L. Walko, 1995: A modeling study of the dryline. *J. Atmos. Sci.*, **52**, 263–285.